AEROACOUSTICS AT THE GERMAN-DUTCH WIND TUNNEL

H. H. Heller, W. R. Splettstoesser, W. M. Dobrzynski, K.-J. Schultz

Institute for Design Aerodynamics
- Technical Acoustics Division -
DFVLR Braunschweig Research Center
Federal Republic of Germany

Abstract

The German-Dutch Wind Tunnel ("DNW") in The Netherlands has been fully operational for about four years. When used in its open test section configuration it represents probably the best aeroacoustic research facility in existence, allowing large scale or even full scale testing of aircraft-related noise generators. This paper attempts to illustrate the unique technical capabilities of the DNW on the example of two major recent research projects, dealing, respectively, with the noise of General Aviation aircraft propellers, and helicopter main rotors. For these two projects, background and technical problem-areas are outlined, the special experimental set-ups - as required in a facility of such physically large size -, the data acquisition and reduction procedures, and the implications of the wind-tunnel-test-obtained results for aeroacoustics are delineated. Also, the preparations for a planned near-term model helicopter main-rotor/tail-rotor aeroacoustic interaction experiment are discussed. Finally, an outlook is given on the DNW-potential for future high qualitiy aeroacoustic research.

1. INTRODUCTION

Aerospace vehicle noise research depends on the experiment. Corresponding efforts may employ (inherently full-scale) flight vehicles which are tested in actual flight, or - if large enough facilities are available and the test object itself is small enough - even in wind tunnels. Here, the NASA-Ames 40' by 80' tunnel, the RAE 24' tunnel, or the Boeing Vertol 20' by 20' tunnel are good examples. Individual noise-generating components of aircraft, such as propellers, rotors or even jet-engines by themselves, on the other hand, may be tested in smaller wind tunnels; here, facilities such as the NASA-Langley 4 by 7 m tunnel, the ONERA 'Cepra 19' 3-m-diam tunnel, the BBN 4' by 4' quiet tunnel, the DFVLR-Braunschweig 1 by 1 m Acoustic Tunnel, the NASA Langley 'Anechoic Flow Apparatus', or the US-Army Moffet Field R&T-Lab "Hover Room" come to mind, to name just a few.

These facilities tend to be characterized by some typical disadvantages: If they are large, they usually suffer from high-level background noise and inadequate anechoic properties of the surrounding test hall; if they have low background noise and good anechoic test hall qualities, then they are usually rather small in size. It now seems, however, that a new facility - the DNW - combines both large physical size and excellent aeroacoustic qualities. (Here DNW stands for "Deutsch-Niederländischer Windkanal", or translated into English, "German-Dutch Wind Tunnel"). Consequently, aeroacoustic researchers flock into this tunnel like moths into the candle-light (and the authors of this paper consider themselves moths too, in this respect), but fortunately, one doesn't get burned in the DNW, but rather only enlightened.

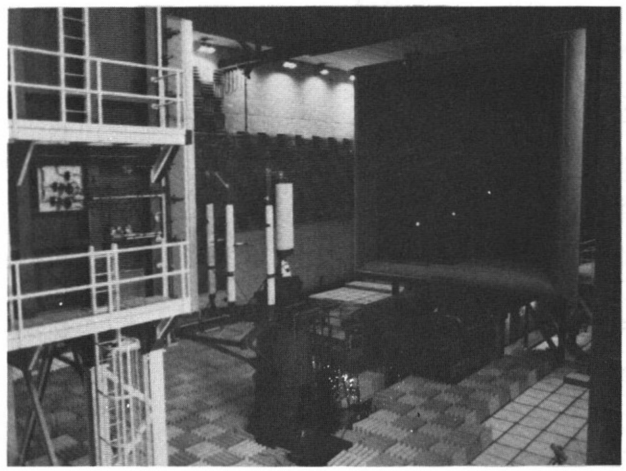

Fig.1 The German-Dutch Wind Tunnel (DNW) in its Open Test Section Configuration

Since the DNW became operational, a number of highly successful aeroacoustic research-projects have been conducted in this facility, mostly by American, Dutch and German research-scientist - sometimes within joint ventures - and two of these shall be discussed in detail in this paper, dealing, respectively with the noise of General Aviation aircraft propellers and helicopter main rotors, the intent being, to illustrate and exemplify the quality of the data obtainable in this new aeroacoustic research facility.

2. THE AEROACOUSTIC QUALITY OF THE DNW

The DNW, which is located in the Netherlands, is jointly operated by DFVLR* and NLR*. As shown in Fig. 1 in its "open test section configuration",

* for all abbreviations, see end of paper

it features a (rectangular) nozzle of 6 x 8 m^2 and a usable length of 20 m between the nozzle and the square (9.5 x 9.5 m^2) collector; the anechoically treated test hall, surrounding the free-jet flow has a total volume of about 27000 m^3. Typical background noise levels, as determined in the flow with a nose-cone-protected microphone are presented in Fig. 2.

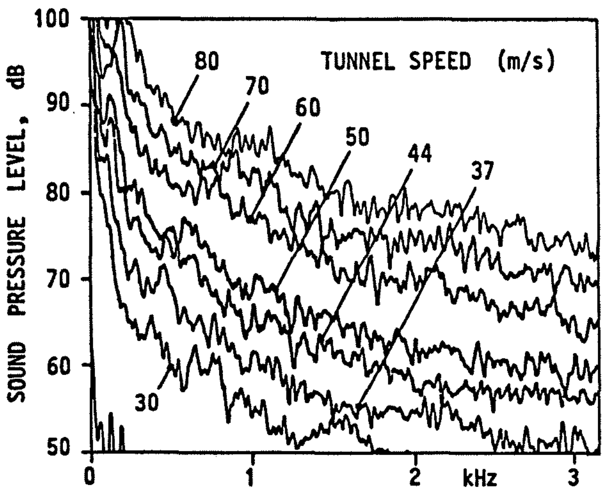

Fig. 2 In-flow-noise Narrow-band Spectra (6.5 Hz Band-width) Measured with Nose-cone-protected 1/4" B&K Microphones

The longitudinal turbulence intensities in the core-flow are shown in Fig. 3. It should be noted that these flow turbulences relate to an open-jet flow, with inherently higher turbulence intensities, as those obtainable within a closed test section flow. Details on the aerodynamic and acoustic qualities of the DNW are presented in /1 - 4/.

3. AEROSPACE VEHICLE NOISE RESEARCH

3.1 Flight Testing vs Wind Tunnel Testing

Fundamentally, aeroacoustic research - specifically on aerospace vehicle related noise generators - serves to improve noise prediction and noise reduction capabilities. For both these objectives, it is necessary to understand the basic noise generating mechanisms and how these ultimately relate to aircraft operational and aircraft geometric parameters. Only then is it possible, to quantify parametric dependences, and to develop techniques to purposely affect the sources for minimum noise generation and/or radiation.

In order to study the very source mechanisms, one should "break down" any particular type of aircraft into its various noise-contributing components. In the case of a propeller-driven aeroplane these might be the propeller, the engine (piston or gas-turbine type), any gears, and the engine-exhaust. To some extent, airframe-noise contributors might deserve special attention. In the case of a helicopter, these might be the main rotor, the tail rotor, again the engine(s) of whatever type, and any gearing. While each of these noise contributors must be looked at on an individual basis, some of these interact: for example, the propeller flow field and its noise-generating process may be affected by the engine-cowling, by wings, or in case of a pusher-configuration by upstream struts or tail-gear. Furthermore, the particular installation of the propeller may also influence the way it radiates sound. A wing or fuselage surface may act as a reflector and hence redirect or even emphasize the sound. Likewise, the tail-rotor of a conventional helicopter operates in the main rotor unsteady wake, within its trailing vortices in particular, or within the wake shed from the main rotor hub. Hence, the interaction of individual noise-contributors is an important additional source of aircraft noise, needing particular attention.

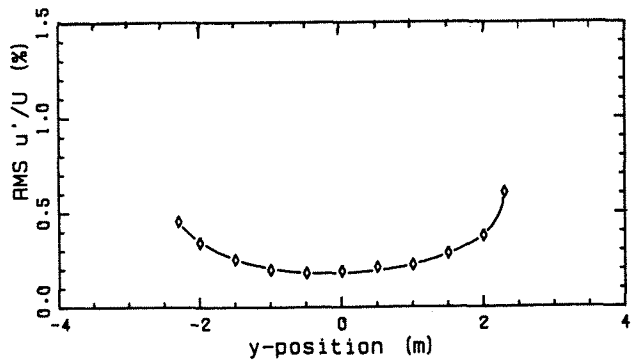

Fig. 3 Lateral Distribution of Normalized RMS-values of the Longitudinal Velocity-fluctuations at a Typical Model Position close to the Center of the Open Test Section (after Michel and Froebel /3/)

Flight testing the actual aircraft in its natural environment inherently yields the most realistic information. Measurements of acoustic signals from a flying object, however, are affected by Doppler-shifts; sound must also propagate through an inhomogeneous and turbulent atmosphere before arriving at a ground-microphone (which may be positioned some distance above ground, inviting assorted ground-reflection problems /5/). Hence, data acquisition, reduction and eventual interpretation is affected by a number of non-source- related influences, causing sometimes severe data-scatter.

Without attempting to discredit flight testing (which of course is indispensable), it must be stated, that well thought-out wind tunnel experiments provide inherently more stable test conditions, allow almost unlimited variation of test parameters and also safe off-design operation. Furthermore, individual aircraft components may be tested by themselves and/or in appropriate combinations.

The draw-backs of wind tunnel testing, of course, are also manyfold: excessive aerodynamic background noise und tunnel turbulence, the proximity of a shear layer to the model, introducing extraneous sound sources, the problem of sound-propagation through the free shear layer, where distortions occur before measurement, the perhaps rather high "lower"-frequency-limit of the absorptive treatment of the test hall walls, and the need of having to employ scaled models with inherent Reynolds-number problems.

3.2 Noise Certification Related Aeroacoustic Research

The motivation for any aircraft manufacturer to develop quiet flight-vehicles is greatly helped by the legislator, who defines and imposes noise limits upon all civil aircraft. Internationally, noise legislation is governed by "Standards and Recommended Practices - Environmental Protection", as laid down in the ICAO-Document "ANNEX 16" to the Convention on International Civil Aviation /6/ where in special Chapters for "propeller-driven aeroplanes above and below certain take-off masses", for "helicopters", and for "subsonic jet aeroplanes" the (noise-certification) test procedures, the noise metrics (such as L_A or EPNL) are spelled out in detail, and take-off-mass-dependent noise limits are specified. Before obtaining a flight operational licence, an operator must acquire an official noise certificate, stating compliance with the noise limit; likewise, any new type of aircraft, or a derived version of an existing type, must obtain a noise certificate.

Corresponding test procedures are carefully developed, field-tested and continuously improved by a special body of ICAO, the 'Committee on Aviation Environmental Protection (CAEP)', which also proposes the noise limits to the Council of ICAO. Both research projects, to be discussed in the following, have either directly been triggered by, or are closely related to certain open questions pertaining to noise certification procedures.

4. PROPELLER NOISE RESEARCH IN THE DNW

4.1 Problem Statement

Recently, ICAO-CAEP has proposed a new procedure for the noise certification of propeller-driven aeroplanes, not exceeding 9000 kg in take-off mass. The new procedure (which is to replace the established one, where the aircraft had to conduct a level overflight at 300 m height above an acoustic ground measurement station) now entails an actual (or simulated) take-off from a "brake-release"-point 2500 m ahead of the measurement station (Fig. 4). The aircraft is to fly with "take-off power" throughout the entire test procedure (until it has overflown the station and the noise levels have dropped by at least 10 dB from the observed maximum), and the maximum A-weighted overall noise-level is recorded. At least four test flights are conducted and the obtained levels averaged for the final noise certification level, which is to be assessed against the noise limit.

The procedure allows testing within a temperature window of 2°C to 35°C, while observed levels must ultimately be corrected towards a reference temperature of 15°C. Although the question of a suitable temperature correction has been debated for at least 10 years (ever since noise legislation for propeller driven aeroplanes was first implemented by ICAO), no universally adopted and ICAO-approved procedure had been developed, most notably, since - even dedicated - flight experiments contained too much scatter, to yield the needed accuracy for the development of a corresponding procedure.

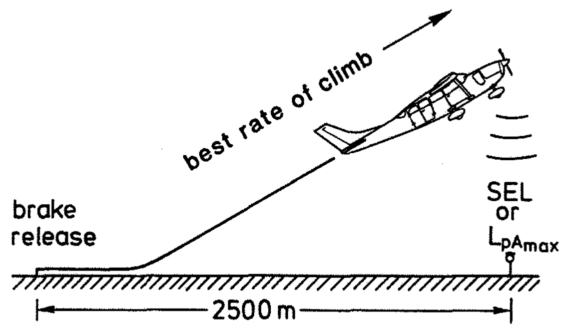

Fig. 4 Proposed ICAO Noise Certification Procedure for Propeller-driven Aeroplanes not Exceeding 9000 kg in Take- off Mass

In flying through the air, the propeller-tip moves in a helicoidal manner and it is well known, that the helical blade (tip) Mach number ("HTM") is the most influential parameter on noise. The HTM, of course, is the dimensionless combination of the speed of sound, the flight (=forward) speed, and the propeller rotational speed; the speed of sound also being a function of ambient temperature. It was thought then, that by varying the rotational speed of the propeller at a fixed ambient temperature one would establish an HTM, which could have also been obtained by keeping both the rotational and the flight speed constant, but varying temperature only. The argument being, that, since it is "solely" the HTM, which affects propeller noise, it should ultimately not matter, how the HTM was achieved, i.e. whether through an RPM-change or through a temperature change. It was this unproven postulate, which hovered around, and was in dire need for substantiation, before a "temperature-correction" on that basis could be officially made a part of any ICAO-CAEP temperature-correction procedure.

Hence, those who advocated a correction procedure, where the dependence of the (A-weighted certification noise) level on HTM could be obtained by flying the aircraft at different propeller-RPMs in order to correct for a test-temperature deviating from the reference-temperature, tacitly assumed that the flow-field around the propeller-tip would be identical in any case, no matter, how the HTM was changed. They further assumed that the relative inclination of the aircraft (i.e. its attitude towards the oncoming mean flow direction) would not vary, even if the propeller-RPM was, say, reduced, and finally, the question of the engine noise contribution and its dependence on any RPM-change was not really dealt with.

Thus, the problem, as it presented itself to ICAO-CAEP was twofold:

(1) Is the noise as radiated by a propeller solely a function of the helical blade-tip Mach-number (rather than of the individual primordial parameters 'flight speed', 'rotational speed' and 'temperature'), thus allowing a temperature-correction on the basis of a "level/Mach-number"-dependence as determined through propeller-RPM changes within a flight test program?

(2) What quantitative effect has a variation in aircraft (and hence propeller rotational plane) attitude on the ensuing radiated noise level, if the aircraft was to change its inclination with respect to the onflow-direction as is to be expected in a climbing-situation?

Within a joint venture, the FAA, the BMV and the DFVLR undertook a dedicated experimental program in the DNW, employing 2 full-scale General Aviation type propellers, essentially with the objective of finding answers for these questions.

4.2 Experimental Approach

(a) Propeller Test Stand

Fig. 5 shows the propeller test stand with the in-flow microphone array and the drive system installed in the DNW open test section, approximately halfway between the nozzle and the collector. The drive system - enclosed within an aerodynamically

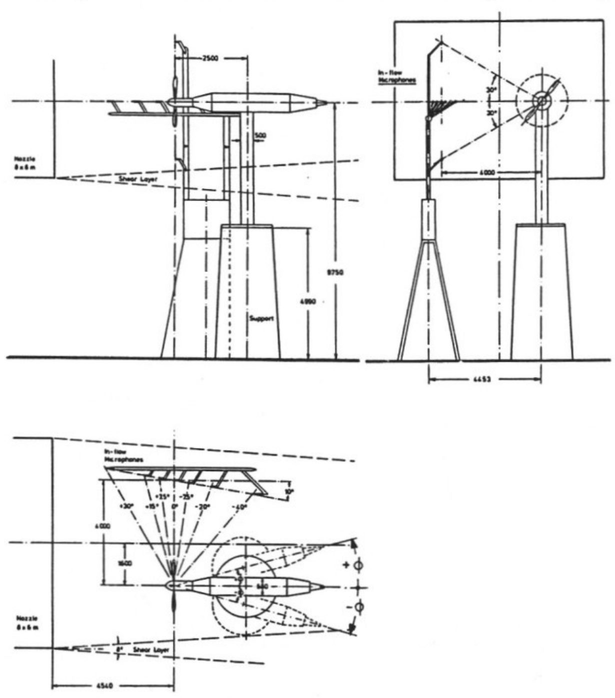

Fig. 5a Schematic of Propeller Test-stand and In-flow Microphone Array

shaped housing of 0.7 m maximum diameter - is located slightly off-center to allow both the propellers and the microphones to be positioned in the (low turbulence) tunnel core-flow region. The distance between the propeller axis and the ("reference") microphone (located in the plane of rotation) corresponds to two propeller diameters. The drive-unit consists of two DC-electric motors (in a tandem arrangement) with a maximum combined

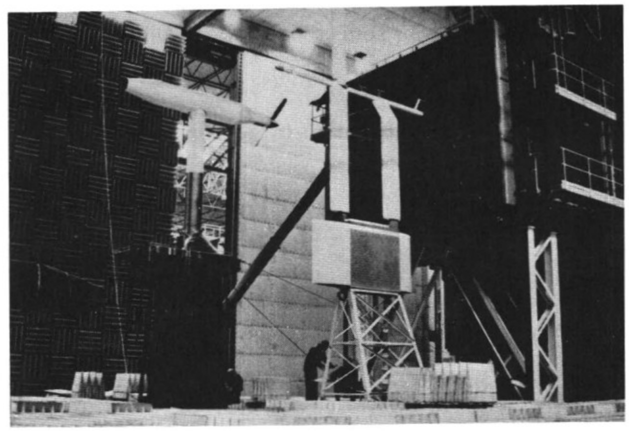

Fig. 5b Propeller Test-stand in the DNW Open Test Section (Flow from right to left)

power output of 360 kW at a rotational speed of 3000 rpm. The central support pylon of 0.5 m in diameter is located 2.6 m downstream of the propeller disc-plane.

Tunnel flow temperature was changed by letting the temperature rise naturally during operation from an initially low value, while the cooling system was inoperative. To realize different propeller disc-plane attitude angles with respect to the tunnel mean flow direction, the entire set-up could be moved (on air- cushions) relative to a ground-fixed center of rotation located directly underneath the propeller center. Appropriate locks in the ground allowed to reproduce any predefined attitude angle within approximately +/-7.5°.

(b) Test Propellers

Two geometrically different 2-blade Hartzell propellers of 2.03 m diameter were tested (Fig. 6), one with a round tip and 6.4% thickness at the 75% radius, the other with a square tip and 8.6% at the 75% radius. Blade pitch was adjusted manually, accurate to within +/-0.2°.

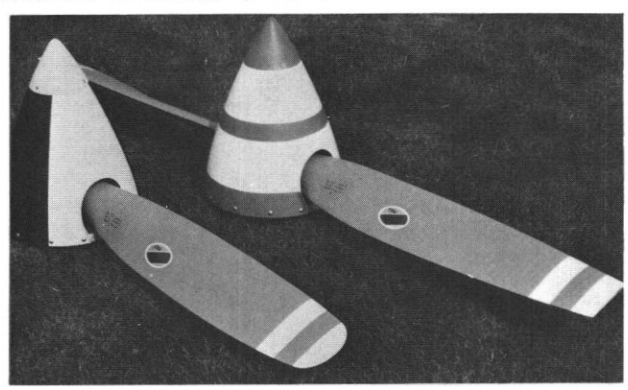

Fig. 6 Test Propellers

(c) In-flow Microphone Arrangement

Seven B&K 1/4-inch-diam. nose-cone-protected microphones were positioned within the low-turbulence core-flow in the horizontal plane at different streamwise locations corresponding to particular geometric radiation angles from the propeller center (see Fig. 5). In order to avoid wake-impingement on a downstream-subsequent microphone, the microphones were arranged in a helically spaced manner.

(d) Reflection Tests

"Bang-tests" served to determine, whether the set-up was susceptible to any sound reflections off nearby structural components with corresponding detrimental effects on the ensuing noise signatures. Explosive charges were attached to the blade-tips, and pressure-time histories at all microphone positions recorded; this procedure was repeated for different blade azimuthal angles.

Two typical pressure-time histories - one where no reflections appear after the initial "bang", and one where two fairly pronounced reflections occur - are shown in Fig. 7. Where, by such efforts,

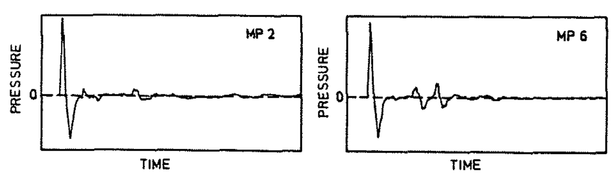

Fig. 7 Examples of "Bang-test"-Results
Left: Absence of Reflections;
Right: Presence of 2 Reflections

"reflecting surfaces" could be identified, they were covered with absorbtive material, which measure usually resulted in a substantial reduction in reflected energy. It was found lateron, however, that even relatively minor reflections affected the time-history wave-forms and spectra; Fig. 8 shows such typical effects.

(e) Propeller-performance and Synchronization

To correlate the acoustic data with propeller operational parameters, the drive system was instrumented with various sensors for thrust and torque (using strain-gauges). Also, rotational speed was monitored by means of an on-axis pulse generator (512 pulses/rev). Synchronization of the azimuthal propeller-blade orientation with the acoustic-data recordings was attained through a "one-per-rev" pulse generator.

(f) Data Acquisition

The microphone output signals were recorded via a multichannel preamplifier system on a 14-channel FM tape-recorder, tape-speed 15 ips, together with the rotational trigger pulses and a time-code signal.

(g) Test Matrix

Within the objectives of the study-program, a test matrix was established to cover

- o a basic test program
- o a test program on the effect of flow temperature
- o a test program on the effect of propeller disc-plane attitude

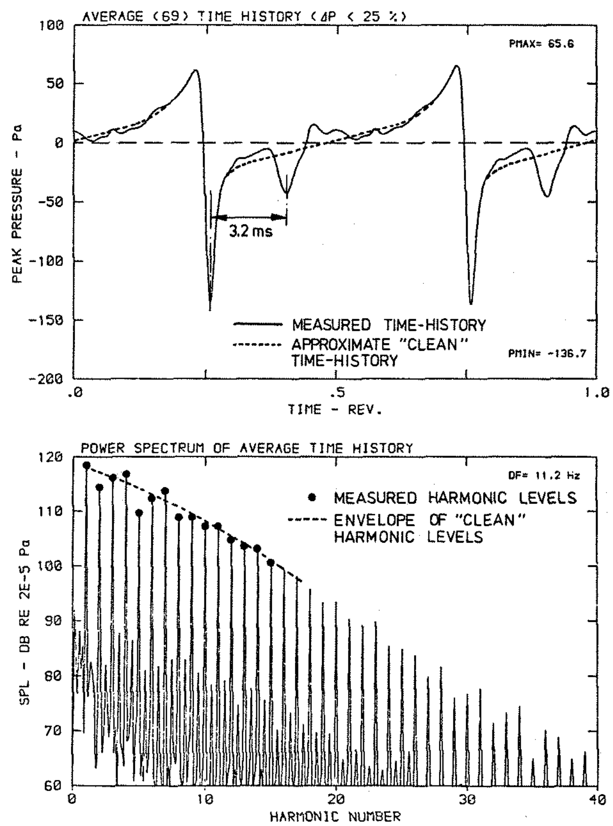

Fig 8 Detrimental Effect of Sound Reflections on a Measured Pressure-time History and Corresponding Narrow-band Spectrum

Within the basic test-program, in essence the blade pitch-angles were changed, to obtain various blade-loadings at otherwise constant advance ratios for a range of helical blade-tip Mach-numbers; here the ambient temperature was kept constant, and the propeller attitude maintained at a zero angle. While in essence repeating the basic test-program, for the temperature-tests the ambient (i.e. flow-) temperature was set at 5°C, 15°C, and 25°; likewise, for the attitude-tests the propeller test-stand was rotated as a whole to the various desired positions, for each of these then going through the basic program-matrix again.

(h) Data Processing

All analogue data-tapes were digitized, whereby the one-per-rev-trigger pulse was used to start the digitization process, with the sample rate corresponding to the 512 pulse/rev.-signal, (which had - during testing - been used to adjust the rotational speed).

To obtain statistically reliable data, averaging is necessary. Therefore, approximately 50 time sequences (corresponding to the time-intervall of 4 revolutions each) were digitized for every data-point and respective pressure-time histories were averaged periodically in the time-domain. By means of an FFT algorithm, pressure level spectra were calculated from all averaged pressure-time histories. All individual harmonic levels were printed out, and this information used to compute both the overall linear, and the overall A-weighted levels, by appropriately adding up all unweighted or weighted harmonics.

The data could then be used for two purposes: First, to determine the dependence of the A-weighted overall levels on geometric and operational paramters, most notably on the ambient temperature, and on the propeller-disc-plane attitude, to help answer the questions posed above in the context of propeller-aircraft noise certification, and, second, to further the understanding of propeller noise generation and radiation mechanisms in general.

The following two sections, therefore, deal with the results on the temperature and the attitude tests, respectively, while subsequent sections discuss the general features of propeller noise, as obtained "as a by-product" in this study.

4.3 Test-results - Temperature-effect

From propeller- and tunnel-operational, as well as tunnel aerodynamic data, such as

- Propeller rotational speed, n [1/min]
- Thrust T [N]
- Torque Q [Nm]
- Power P (equal to $Q \cdot 2\pi \cdot n/60$)
- Wind-tunnel flow velocity v [m/s]
- Absolute Pressure p [Pa]
- Temperature t [K]
- Relative humidity φ [%]
- Blade tip speed, u [m/s]

the advance ratio ($\lambda = v/u$), the helical blade-tip Mach-number and the dimensionless propeller power-coefficient c_P was calculated; here

$$c_P = \frac{P}{(n/60)^3 \, D^5 \, \rho}$$

(where ρ is the air-density at the prevailing air-temperature and humidity, and D is the propeller-diameter).

Tests conducted for several different blade pitch angles (but at constant temperature) revealed that the (A-weighted) overall propeller noise levels can be normalized with the 1.5th power of the propeller power-coefficient c_P. All measured levels - when plotted vs the helical blade-tip Mach-number - then follow one well-defined data-curve. Hence each propeller exhibits its own individual such "curve".

These ensuing basic relationships between noise level and Mach-number - which are valid in that particular form however only for radiation in the plane-of-rotation and a small range of angles in the forward and rearward arc - are now used as a reference to check the influence of flow-temperature.

In Fig. 9 data as measured at different flow-temperatures are plotted versus helical blade-tip Mach-number both for the round-, and the square-

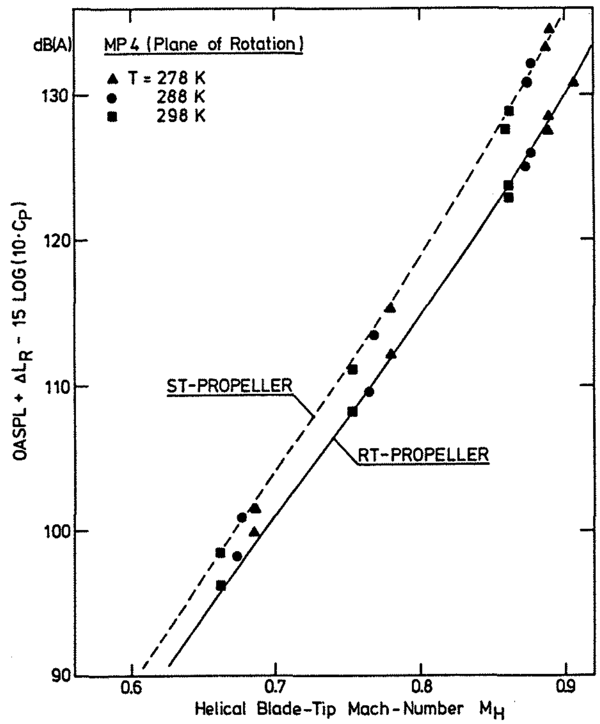

Fig. 9 Helical Blade-tip Mach-number Dependence of Normalized Overall A-weighted Noise Levels Measured Two Propeller-diameters to the Side in the Plane of Rotation

tip propeller. It is obvious, that in this case too, all data points follow exactly the "basic" curve of each propeller (which curves themselves are based on a large number of data-points, as obtained during the basic test-program).

This result now strongly suggests, that there is no additional temperature effect other than that implied in the general noise level dependence on helical blade-tip Mach-number.

It should be emphasized again, that this conclusion is only valid for data which had been normalized beforehand on the basis of a 1.5th power of the "propeller-input"-power-coefficient. Also, for otherwise invariant operational conditions, a "low-temperature environment" tends to slightly increase the blade-loading, while a "high-temperature environment" decreases such loading. Still, within the temperature range of interest for noise certification, such minor blade-loading variations could at most cause level differences of up to 0.5 dB(A).

More importantly, however, it now seems, that it would indeed be a viable approach to derive a "correction-curve" by means of repeated flights at different propeller-rotational speeds, thus establishing a noise-level-vs-Mach-number-dependence, which could ultimately be used to correct data from measuremnent temperature to reference temperature, provided there was no significant engine noise contribution.

On the other hand, since the data indicate, that the slopes of both curves, as shown in Fig. 9 for the two test-propellers of different blade-thickness and tip-shape, are not too different, one could simply take a mean-slope for purposes of "noise-level/temperature"-correcting all propellers, independent of their geometries and also the number of blades. Such an approach would certainly be more than adequate for noise certification purposes; in this case one could dispense with any additional test-flights (of various propeller-RPMs) alltogether. A corresponding proposal has been made to the ICAO-CAEP /7/ for introduction into the new light-propeller-aircraft noise certification procedure.

4.4 Test-results - Attitude-effect

Comparing noise data, which were measured in the plane-of-rotation for zero-, and non-zero-attitudes, showed levels to increase for positive, and decrease for negative, values of the attitude angle (definition as indicated in Fig. 5a).

Assuming now, that the "effective noise source" was tied to that particular propeller-blade which advances towards the microphone, it becomes obvious, that positive attitude angles must cause an increase (and negative attitude angles a decrease), in the local effective blade pitch angle, and also in the local helical blade-tip Mach-number (which effect could - in analogy to the aerodynamics of a helicopter rotor - be termed an "advancing blade tip"-effect).

For the particular instant in time where the propeller blade axis is orientated at right angle to a connecting line between the propeller hub and the microphone, the corresponding deviations in blade angle-of-attack and Mach-number may now be calculated in terms of attitude angle and advance ratio. Results of a corresponding calculation are plotted in Fig. 10.

Hence, for a typical advance ratio λ of, say, 0.25 and an attitude angle ϕ of +7 deg, for example, Fig. 10 would indicate an increase in local angle of attack of about 0.8 deg and at the same time a rise in Mach-number of about 3 %. From the measured relationship between angle-of-attack and power-coefficient for each propeller, one may then determine, that a 0.8 degree difference in angle of attack would result in a level-increase of not more than 0.6 dB(A). Due to the extreme sensitivity of noise radiation towards helical blade-tip Mach-number changes, a 3 % Mach-number increase on the other hand raises the observed noise level by some 3.5 dB(A), as may be seen from Fig. 9.

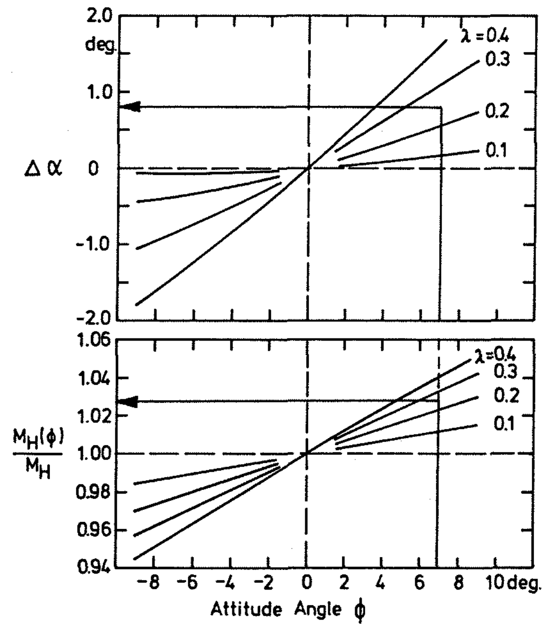

Fig. 10 Propeller Disc-plane Attitude Correction for Angle of Attack and Helical Blade-tip Mach-number with Reference to a Zero-attitude Condition

One may now plot noise levels, as they are measured for different attitude angles versus a "corrected (i. e. local) Mach-number", as shown in Fig. 11 (disregarding, however, any blade-loading correction). Excellent agreement is achieved for Mach-numbers in excess of 0.7, since all data-points fit again the same "general curves" for, respectively, both propellers, which had been obtained in the basic part of the test program. In essence, one finds that the proposed correction procedure could successfully be applied to those noise signatures which are governed by thickness-noise radiation.

Therefore, attitude effects as observed near the plane of rotation can be corrected in a straightforward manner for any given advance-ratio and attitude angle, if for the propeller under consideration, the dependence of the A-weighted noise levels versus helical blade-tip Mach-number is known in advance. Such general curve may be determined for the propeller-disc at zero-attitude, and no specific attitude-change-tests are necessary.

4.5 Loading-Noise and Thickness-Noise

The results presented in the previous sections seemingly showed no break in the slope of the overall A-weighted propeller noise levels, when plotted against an (albeit normalized) helical blade-tip Mach-number. This may simply be coincidental, since - although a rise in helical blade-tip Mach-number increases the number of rotational harmonics and their respective intensities towards higher harmonics - the "smoothing" effect of

A-weighting may also smooth the level-vs-Mach-number-curve, thus in the end allowing the establishment of relatively simple temperature (and also attitude-) correction procedures.

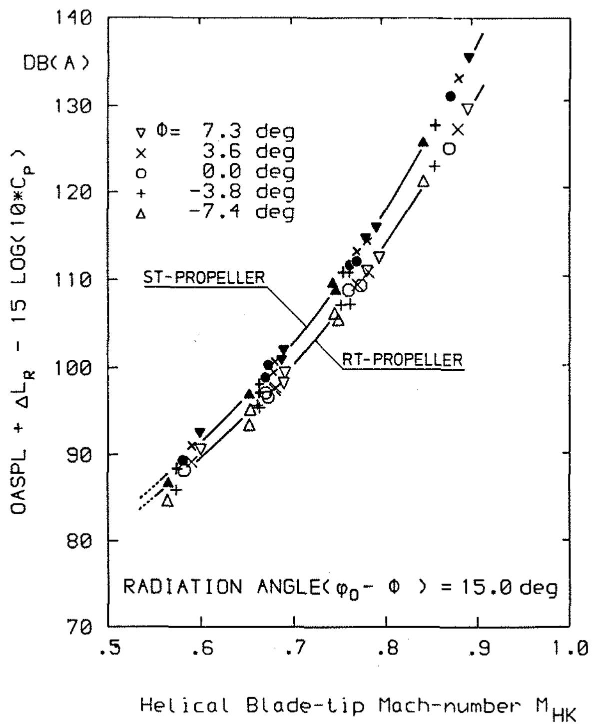

Fig. 11 (Attitude-) Corrected Helical Blade-Tip Mach-number Dependence of Normalized Overall A-weighted Noise Level Directional Maxima, Measured Two Propeller-diameters to the Side

It is of course known, that the two dominant propeller noise mechanisms, namely blade-thickness and blade-loading, express themselves differently in the pressure-time wave-forms, and directivity characteristics.

Singling out the blade-loading effect, by keeping HTM, and advance-ratio constant, but varying the power-coefficient by a factor of 10 (through an appropriate change in blade-pitch), significantly affects the pressure-time wave-form. Fig. 12 shows a corresponding result for the square-tip propeller at a medium test-HTM of 0.72, as measured in the plane-of-rotation. Both wave forms are different in terms of the ratio of positive-to-negative pressure amplitudes and the instances-in-time, for which the respective pressure mimima occur. In agreement with theory, this result is a consequence of the predominance of a pronounced negative pressure pulse in case of diminishing blade-loading, i.e. if thickness-noise dominates the total noise signature. At the same time, this pressure *minimum* of a *thickness-noise time history* is known to occur at roughly the zero-pressure crossing instant of a loading-noise-dominated pressure signature.

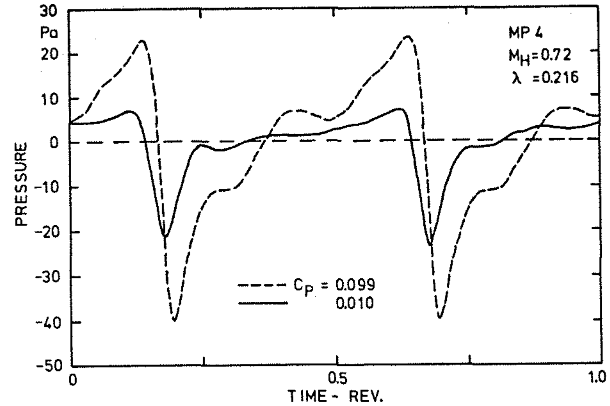

Fig 12 Pressure-time Wave-forms for High and Low Power-coefficients as Measured in the Plane-of-rotation for a HTM of 0.72 and an Advance-Ratio of 0.216

A similar change in blade-loading, corresponding to a power-coefficient variation from 0.01 to 0.13 shows a fairly pronounced effect on the levels for the blade-rotational fundamental frequency (HN = 1) and a low harmonic (HN = 4), while there is next to no influence for a higher harmonic, the 7th in the case shown (Fig. 13). This behavior demonstrates that - in the plane-of-rotation - loading-noise most strongly affects the fundamental and low blade-harmonic frequencies, while higher harmonics here are essentially independent of the blade-loading, and determined entirely by blade-thickness.

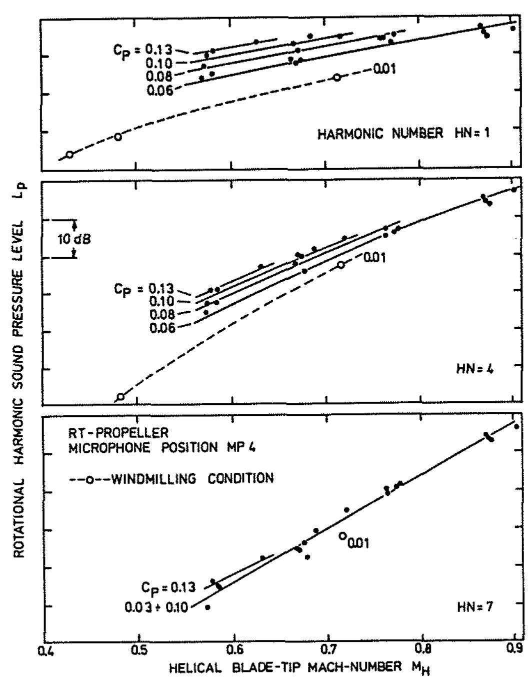

Fig. 13 Helical Blade-tip Mach-number Dependence of the Levels of the Blade-rotational Fundamental (HN = 1), and Higher Harmonics (HN = 4 and HN = 7) for Various Power-Coefficients

5. ROTOR NOISE RESEARCH IN THE DNW

5.1 Problem Statement

Helicopter noise represents a growing environmental problem since its characteristic features makes it highly annoying. Noise legislation in terms of an ICAO-"Standard" for noise certificating helicopters was first introduced in 1981 (ANNEX 16/Chapter 8), but some uncertainties in the certification procedures, caused a debate on the proposed noise limits, being considered either too severe or too lenient, depending on whose opinion was asked.

Both the main- and the tail-rotor are individual noise-sources with their own characteristic source-mechanisms; the tail-rotor, furthermore, operates in the main rotor wake, and this main-rotor/tail-rotor interaction constitutes an additional annoying and easily recognizable source of helicopter noise.

One particular area of uncertainty pertains to the occurrence (and the control for that matter) of helicopter impulsive noise, the characteristic "blade-slap", that makes helicopter noise discernible over large distances. Attempts to accurately predict the onset, and/or the regimes, within which impulsive noise would occur for any given rotor have largely failed, due to the insufficient quantitative understanding of the impulsive-noise dependence on rotor-geometry and -operation. Hence, only empirical schemes were developed to enable - with an uncomfortably large margin of uncertainty - the prediction of blade-slap occurrence.

Impulsive noise is known to occur especially during high speed forward flight (where compressibility effects predominate near the blade tips), and certain phases of descend and landing approach (where the blades may cut through previously shed vortices) (Fig. 14).

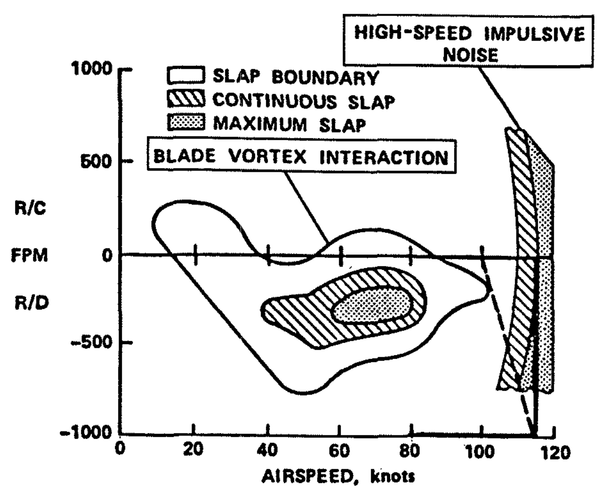

Fig. 14 Typical Regimes of Impulsive Noise Occurrence as Function of Forward Flight Speed and Rate of Climb (after Cox /8/)

Noise certification procedures, as laid down as a "Standard" in ANNEX 16/ Chapter 8 /see Ref. 6/, require the helicopter to be noise tested during take-off, level-flight, and landing-approach.

If a helicopter was certification-tested in an operational regime (not necessarily corresponding to its preferred mode of flight), where impulsive noise would occur during any of the prescribed certification-procedures, it would be judged noisy. Another helicopter, which was to operate outside such critical regimes during certification testing, would be judged quiet. The onset of impulsive noise under straight-level flight conditions is rather sudden and tends to increase rapidly in intensity with growing flight speed (Fig. 15). Likewise, the occurrence of impulsive noise during descent is restricted to a fairly narrow range of flight-speed/rate-of-descent combinations (see Fig. 14). To develop just noise certification procedures and corresponding noise limits, - especially for the level-overflight- and the approach- test, a thorough understanding of onset-conditions and operational regimes for any given helicopter (main rotor) is necessary. Such understanding is also instrumental, to allow for an increase in flight speed for new-design helicopters without excessive noise penalties, or to specify such flight regimes during landing approach, where impulsive noise would definitely be absent.

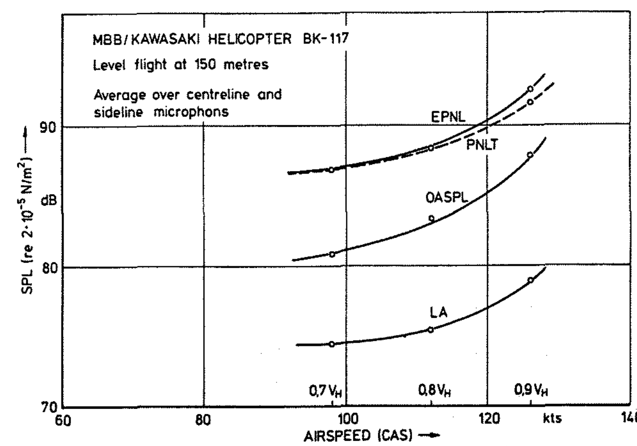

Fig. 15 Typical Flight Speed Dependence of Noise Level during Certification Testing (from /9/)

Much as flight tests would be suited to most realistically look into relevant problems - and numerous corresponding studies have been conducted in the past /9-11/ -, wind tunnel tests again lend themselves for systematic and probably rather more accurate investigations, inherently allowing wider and better controllable variations of pertinent parameteres, as long - however - as scaling problems are recognized and fully understood.

The problems to be resolved could thus be formulated in the follwing manner:

(1) What are the characteristic features of (a) high speed impulsive noise, and (b) blade/vortex-interaction impulsive noise, and can these be studied in scaled wind tunnel tests?

(2) How well do wind tunnel model test results on rotor impulsive noise (both for high speed conditions, and for conditions of blade/vortex interaction) scale with flight test results?

(3) How accurately may farfield radiated impulsive noise (for purposes of predicting noise certification levels) be computed from geometrical and operational parameters on purely theoretical grounds?

(4) What role plays the tail rotor contribution in the total noise signature, specifically for noise certification EPN-levels, and - more generally - in the helicopter detectability at large distances?

To adress the first three of these questions, a comprehensive experimental/analytical effort was launched in the DNW within a joint effort of the US Army Aeromechanics Laboratory (AVSCOM) and the DFVLR /12 - 14/. To try and answer the fourth question, dedicated experiments are currently undertaken in the DNW, to be briefly discussed in Section 6.

5.2 Experimental Approach

(a) Rotor Test Stand

The rotary wing test stand (RWTS) of the Aeromechanics Laboratory - a photograph of the set-up is shown in Fig. 16 - was positioned in the open test section of the DNW, with the rotor-hub located mid-way between the nozzle and the collector, and 10 m above the acoustically absorbtive tunnel floor. The RWTS was driven by a 400 Hz variable frequency, 90 hp electric motor. The rotor itself was mounted on a teetering hub assembly with rotor controls (collective, and longitudinal and lateral cyclic) provided by a remotely-controlled swashplate actuator, allowing also a direct rotor-tip-path-plane control. The entire assembly was mounted on a six-component strain gauge balance for thrust, drag and pitching-moment determination.

(b) Model Rotor

A 1/7-geometrically scaled 2-blade rotor - corresponding to an AH-1 series helicopter ("Cobra") with OLS ("operational loads survey") blades was mounted on the RWTS. The model rotor diameter of 1.916 m corresponding to one-fourth and one-sixth, resp., of the DNW nozzle width and nozzle height, resp., could thus be positioned well within the clean, low-turbulence core-flow regime. One blade was instrumented with 32 flush-mounted Kulite absolute-pressure transducers, the other with 18 differential-pressure transducers, located essentially along the leading edge and at several chord-positions in the blade-tip region.

(c) Microphone Arrangements

Ten B&K 1/4-inch-diam. nose-cone-protected condenser microphones inbedded in foam-layered adapters were positioned on individual support struts at several distances upstream, either in the plane of rotation, or 30° and 45° downward of the rotor hub, still well within the core-flow. There were also several out-of-flow microphones.

(d) Acoustic-reflection Prevention

"Bang-tests" were conducted for similar reasons as outlined in Section 4.2.(d); accordingly, most all support struts for the microphones, and also the very support pylon for the rotor hub had to be wrapped with absorbtive material, since large reflecting areas were found to otherwise detrimentally affect the radiated noise signatures.

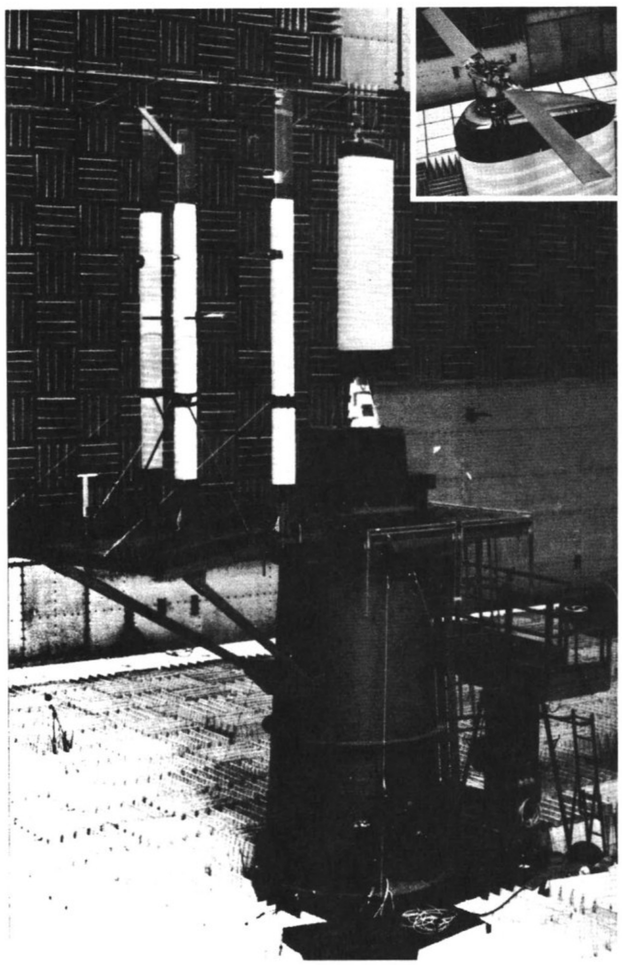

Fig. 16 Model Rotor Test Set-up in the DNW Open Test Section. Insert: Close-up of Two-blade Rotor

(e) Data Acquisition

Three multichannel FM tape recorders were used for blade-surface pressure, and acoustic pressure recordings, operating at 30 ips for recording frequencies up to 20 kHz. To assure synchronization between the recorders, an IRIG-B time code and azimuthal rotor-shaft position related pulses were recorded simultaneously on all three tape recorders.

Two double-channel FFT-analyzers permitted on-line analysis of 4 selected channels. Tunnel operational data were recorded and/or noted independently for each data-point.

(f) Test Program

Within the program-objectives, there were essentially two test phases, comprising simulation of high-speed impulsive noise, and blade/vortex-interaction impulsive noise, respectively. Data were to be compared to available full-scale data from a thorough flight test program on a Cobra helicopter conducted by the US-Army /15 and 16/. Here, the test helicopter flew in formation with a quiet propeller-aircraft, equipped with microphones, such that helicopter rotor acoustic radiation could be measured at any desired relative position around the test vehicle. The test matrices for the DNW-tests thus were to cover those test-parameter variations, that had been obtained in flight.

For the model-tests, certain combinations of the tip-path-plane angle and the advance-ratio (of the blade during its advancing phase) do correspond to certain rates of climb (or descent), and to certain straight-level forward flight speeds for the full-scale flight situation; the tunnel test matrix was therefore to duplicate the corresponding full-scale flight conditions, as shown in Fig. 17.

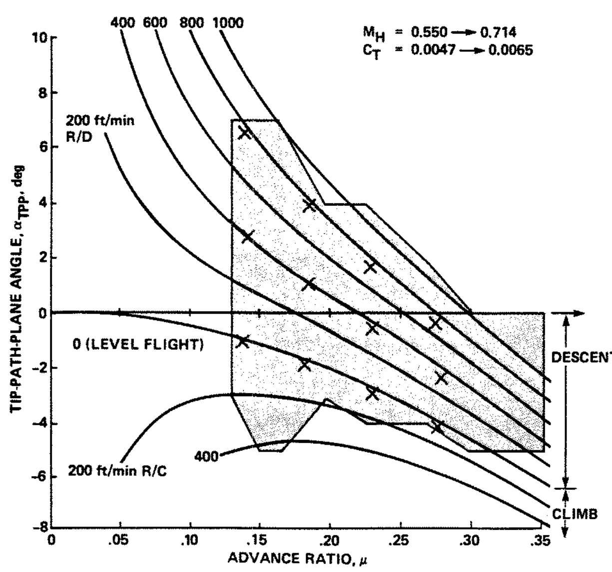

Fig. 17 Operational Envelope for DNW-tests

The rotational blade-tip Mach-numbers, that could be achieved in the tunnel, ranged from approximately 0.55 to 0.72, resulting in advancing tip Mach-numbers of up to 0.92. Equating the important (non-dimensional) parameters, namely rotational Mach-number, advance-ratio, as well as thrust-coefficient in the model tests to those of the full-scale flight conditions, and furthermore adjusting the tip-path-plane angle such that any desired rate-of-climb or straight level flight condition was duplicated in the tunnel tests, assured direct comparibility of full-scale and model-scale data.

(g) Data Processing

In essence, all (recorded) anti-aliasing-filtered analogue-data were A/D-converted, triggered by both a time-code signal and a 1/rev.-signal. On-line checks and off-line data analyses were conducted in a similar manner as outlined in Section 4.2 in the context of the propeller-noise tests.

Pressure time histories of acoustic events in the case of rotor aeroacoustic research, are rather more informative, than spectra. While flight data are inherently fairly unstable (atmospheric turbulence, flight-control variations, distance changes between test and observer aircraft, etc), DNW-tunnel test data were found to be extremely stable. Hence, in the first case, data averaging is imperative. Also, a technique, developed by Boxwell /15/ to extract a main rotor noise signature from an unstable, and tail-rotor noise contaminated, signature, was necessary in the analysis of flight data. This technique makes use of appropriately strong spikes within the acoustic signature itself for triggering the analysis process, by which method an extremely clear and "noise-free" signature of the main-rotor flight noise signature is obtained. This clean signature is now very well suited for comparison with scaled tunnel test data.

5.3 Test Results - Blade/Vortex Interaction Noise

The left column in Fig. 18 illustrates the effect of such processing of full scale flight data: Here, the top-, and the middle-frame show unaveraged data, as they occur for nominally constant flight conditions. Clearly, the wave-forms and the amplitudes are rather different; also, the higher-frequency periodic components of the tail rotor are clearly visible between the dominating BVI-spikes. Applying now the above processing technique with "spike-triggering" and averaging, produces the bottom frame, now very clearly exhibiting the BVI-waveform-features without any tail rotor contribution.

The right part of Fig. 18 now shows the corresponding and appropriately scaled data from the tunnel tests. Firstly, the top (instantaneous) and the bottom (multiply averaged) waveforms are virtually identical (illustrating the extremely stable tunnel flow conditions). Secondly, the full-scale flight waveform, and the scaled tunnel test waveforms are very similar, indeed.

Fig. 18 was to essentially illustrate the procedure, that allows a physically meaningful comparison of full-scale and model-scale data, (showing the time span of one full rotor revolution with two major spikes, one for each blade). The particular features of impulsive, specifically of BVI-impulsive noise, become more obvious in Fig. 19. Here, "looking down from above" onto the rotor, one observes in the top-row (where in-plane forward radiated waveforms are shown) in essence

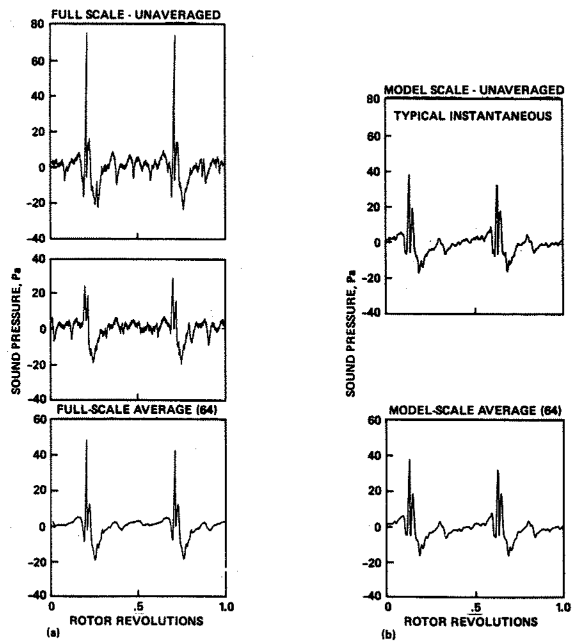

Fig. 18 Unaveraged and Averaged Pressure-time Histories for Full-scale Flight (left) and Model-scale Tunnel (right) Tests for a BVI-condition

negative spikes, while in the bottom row (corresponding to a forward, 30°-downward radiation) positive spikes predominate. These latter ones are

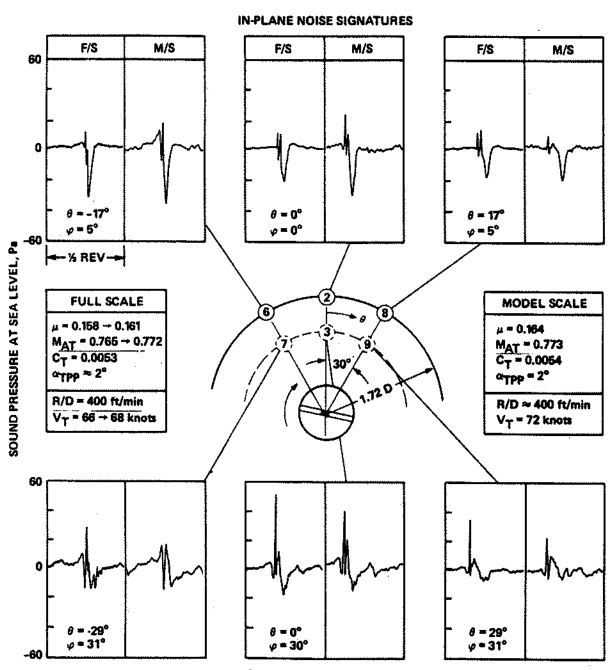

Fig. 19 Full-scale Flight (F/S) and Model-scale (M/S) Pressure-time Histories for In-plane (top row) and Downward-forward (bottom row) Radiation under Impulsive Noise Conditions

to be interpreted as blade/vortex-interaction caused, known to prodominantly radiate into a downward/forward direction. The "in-plane"- negative spikes, on the other hand, as shown in the top row, are related to thickness effects. Also, in this presentation, each two neighboring frames correspond to each other, where F/S stands for full-scale flight, and M/S for model-scale test results.

5.4 Test-Results - High-speed Impulsive Noise

The data, as depicted in Fig. 19 actually had shown a BVI-noise dominated case, with a fairly low advancing tip Mach-number (approximately 0.77) and an actual (or simulated) rate-of-descent of 400 ft/sec.

Considering now the acoustic signatures for a situation of straight-level high-speed flight with an advancing blade-tip Mach-number of 0.84 (Fig. 20) as observed in the forward plane of rotation and in a downward/forward direction, the ensuing pressure signatures are now all characterized by strong negative spikes, more intense still in the rotaional plane; this is consistent with the understanding that high speed impulsive noise is most pronounced in the rotational plane. Again, the similarity of full-scale flight (F/S) and model-scale wind tunnel (M/S) waveforms is rather striking, exemplifying the excellent scaling of model towards full-scale data.

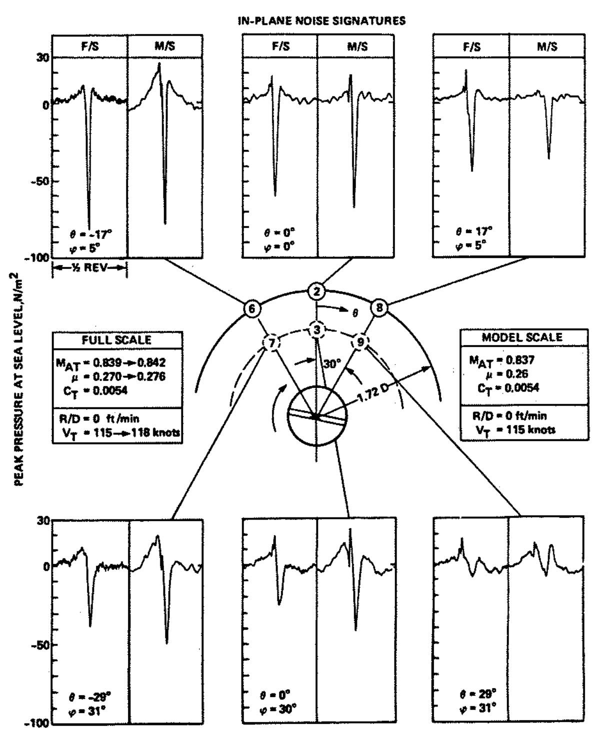

Fig. 20 Full-scale Flight (F/S) and Model-scale (M/S) Pressure-time Histories for In-plane (top row) and Downward-forward (bottom row) Radiation under High Speed Impulsive Noise Conditions

5.5 In-between Considerations

Based on the results, as presented in Sections 5.3 and 5.4, one may well positively answer the first two questions as posed at the end of Section 5.1: firstly, the gross and even also rather detailed features of (full-scale) helicopter rotor impulsive-noise pressure-time history waveforms are very well duplicated in the DNW, provided careful data analysis and processing are employed; secondly, scaling for impulsive noise works very well, even with an, after all relatively small, seventh-scale, model of a helicopter main rotor.

Attempting to compute such waveforms from first principles, however, seems not possible. Computation of the unsteady blade-surface pressure field for either the high speed flight case or the rapid descent case has not successfully been attempted. Computing, however, acoustic radiation into the farfield from known blade-surface pressure characteristics, seems rather more promising. It was for this reason, among other things, that surface pressures were measured in detail within the subject test program.

5.6 Test Results - Blade-surface Pressures

To relate the farfield-radiated acoustic signatures (as shown in Figs 19 and 20 above), to the originating time-varying blade-surface pressures, corresponding time-histories, as measured by means of one each upper-, and lower-surface located pressure sensor during one revolution, are shown in Figs. 21 and 22. The respective sensors, which were flush-mounted in the blades, were located very close to the leading edge (3% chord-position) and the blade-tip (97.5% blade station). Fig. 21 then shows the surface pressure-time history on both blade surfaces for conditions corresponding fully to those in Fig. 19 above, i.e. for a situation, where essentially blade/vortex interaction occurred; clearly there seem to be three encounters of the blade (tip) with vortices, as obvious from the rather steep gradients in the pressure signature. It should be remembered, that it is of course the time-varying difference in the lower and upper surface pressure signature, which yields the lift variation during one revolution, and which must be obtained (and integrated) over a sufficiently large blade area to represent the acoustic source, whose radiation is ultimately observed at some farfield point.

Fig. 22 presents corresponding results for the high-speed impulsive noise case, as had been shown in Fig. 20 above, again for the same pair of blade-surface sensors.

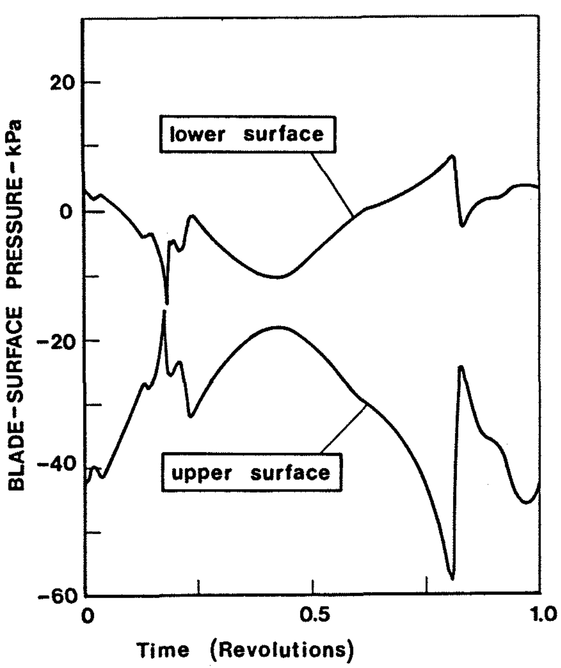

Fig. 21 Blade-surface Pressure Time-histories During One Rotor-Revolution for an Upper-, and a Lower-Surface Position Close to the Leading-edge and the Blade-tip for Experimental Conditions of Blade/Vortex-Interaction Impulsive Noise Identical to those Depicted in Fig. 19 (M_{AT} = 0.77)

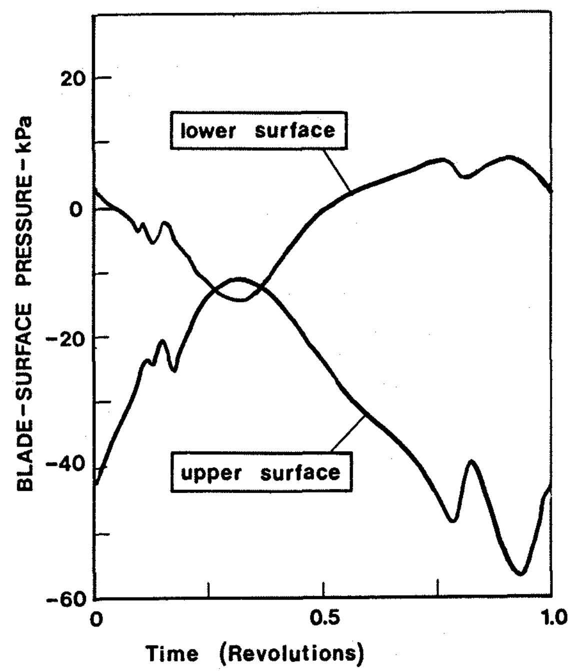

Fig. 22 Blade-surface Pressure-time Histories During One Rotor-Revolution for an Upper-, and a Lower-Surface Position Close to the Leading-edge and the Blade-tip for Experimental Conditions of High-speed Impulsive Noise Identical to those Depicted in Fig. 20 (M_{AT} = 0.84)

Similar results have been obtained for a large variety of operational conditions, and blade locations, such that a data bank is now avaiable, which can be used to develop and/or verify prediction schemes, relating unsteady blade-surface pressures to radiated impulsive rotor noise.

One such example is shown in Fig. 23, where essentialy on the basis of the "Ffowks-Williams/Hawkins"-equation /17/ blade-surface data were used by one of the authors (Schultz) to calculate the radiated acoustic time history at some farfield point. The procedure employed accounts for both the thickness-noise and the loading-noise-contribution.

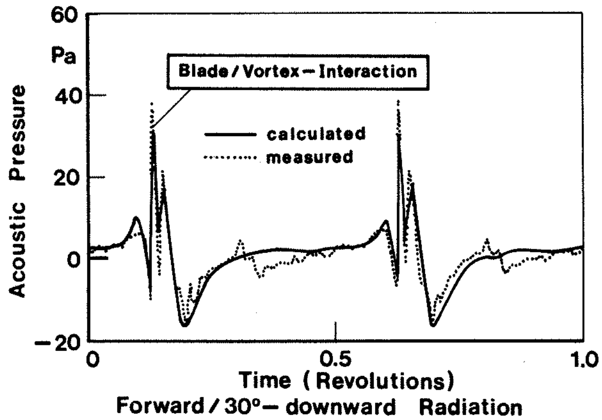

Fig. 23 Farfield-observed Blade/Vortex-Interaction Noise Pressure-time History: 'Calculated' on the Basis of Measured Blade-surface Pressure-time Histories and 'Measured' in the Wind Tunnel Experiment (for Conditions Corresponding to Fig 19, bottom-row/center-frame M/S)

Hence, to answer the third question, posed at the end of Section 5.3, one must state, that the computation of impulsive noise from rotors just on the basis of geometrical and operational data does not seem feasable yet. Having however available experimental blade surface pressure data, then farfield radiated noise may be computed on that basis.

6. FUTURE AEROACOUSTICS PROJECTS

Based on the highly successful outcome of the experimental research projects on aircraft propeller noise and on helicopter main rotor noise, as described above, there are plans for further utilization of the DNW as a prime aeroacustic research facility. Several projects are in the planning stage, or even in the phase of execution.

6.1 Large-scale Rotor Testing

The main rotor tests utilizing a 1/7-scale model rotor, suggested rather excellent scaling towards full-scale. In some operational regimes (not reported in this paper), however, some less good scaling was observed, especially during blade/vortex-interaction. It is suspected, that the relative core-size of the shed vortices, did not properly scale, causing different results for model- and full-scale.

Therefore, a test-program is currently underway in the DNW, using a DFVLR 1/2.5-scaled 4-blade main rotor corresponding to a BO-105 main rotor. Within a joint NASA-Langley/DFVLR research project, tests are being conducted, which, among other things, pertain to blade/vortex-interaction noise; results are to be compared to full-scale flight tests on a BO-105 planned by DFVLR in the near future to assess again scaling details, this time however for a modern hingeless 4-blade rotor, rather than the previously used stiff 2-blade rotor.

6.2 Main-Rotor/Tail-Rotor Interaction

As delineated further up, the role of the tail rotor in the acoustic signature of a helicopter is not fully understood in its effect on helicopter detectability and on the final noise certification levels within the 3 test-procedures. One major area of uncertainty in the latter context pertains to its influence at high speed forward flight (one of the certification procedures) on the ensuing noise signature. Correcting an EPN-level from test- to reference-flight-speed requires the "noise-sensitivity"-(with flight speed)-curve for the helicopter, which is - of course - affected by both the main-, and the tail rotor. Corresponding corrections are normally based on the main-rotor advancing tip Mach-number alone. If the tail rotor tip Mach-number was to markedly differ from that of the main rotor, for example, then the tail rotor might exhibit an influence not related to the main rotor advancing tip Mach number. Hence the need, among other things, to study tail-rotor aeroacoustics in detail.

A corresponding research project in the DNW is currently conducted by DFVLR, where a 1/2.5-scaled model tail rotor, fully compatible with the DFVLR model main rotor, is tested as a combined system. The tail rotor is instrumented with 20 flush-mounted Kulite sensors, to allow acquisition of time-varying blade surface pressures for the tail rotor operating by itself, or in the wake of the main rotor.

6.3 Propeller Noise Tests

While no specific propeller noise research project is planned in the DNW by DFVLR at this time, considerations towards future studies center about the effect of disturbed inflow into the propeller rotational plane, a situation which typically occurs for a pusher-propeller configuration. Here questions on optimum positioning of upstream struts or wings for minimum noise generation are of considerable interest.

7. OUTLOOK

The German Dutch Wind Tunnel has repeatedly proven to be one of the - if not the - foremost aeroacoustic research facility in the world. Research projects on propeller noise and rotor noise, such as those reported in this paper (and others, not reported in this paper), have yielded high quality data, perhaps of benchmark quality. Every new aeroacoustic project provides additional insight into the DNW's capabilities, and the planning and execution of new projects gains from the ever growing experience, obtained through numerous fruitful - frequently international - cooperative efforts.

The development of new helicopters, of propeller-driven aeroplanes with tractor or pusher propellers, of jet-aeroplanes, and of propfan-propulsion systems may depend and would undoubtedly greatly benefit from the existence and availability of the German Dutch Wind Tunnel.

BIBLIOGRAPHY

/1/ Schultz, K.-J.: "Der Deutsch-Niederländische Windkanal als aeroakustische Versuchseinrichtung", DFVLR- Nachrichten, Heft 34, Nov. 1981

/2/ Michel, U.; Froebel, E.: "Turbulence Levels in the German-Dutch Wind Tunnel", DFVLR Interner Bericht IB 22214-82/B2, Jan. 1982

/3/ Michel, U.; Froebel, E.: "Turbulence at Far Downstream Positions in the Open Working Section of the DNW", DFVLR Interner Bericht IB-22214-85/B10, 1985

/4/ Ross, R., et.al.: "Aeroacoustic Calibration of DNW Open Jet, DNW TR 82.03, July 1982

/5/ Dobrzynski, W., "Interferenzwirkung durch Bodenreflexion bei Fluglärmmessungen an Propellerflugzeugen", DFVLR-Forschungsbericht, FB 81-28, 1981

/6/ International Standards and Recommended Practices ENVIRONMENTAL PROTECTION; ANNEX 16 to the Convention on International Civil Aviation, Aircraft Noise, Vol. I, First Edition - 1981

/7/ Dobrzynski, W., "Propeller Blade-Tip Mach-Number Correction From Measurement to Reference Conditions". Background Information Paper BIP No. 6, ICAO-CAEP Working Group II Meeting, Ottawa, Can., Oct. 1985, and DFVLR Interner Bericht IB 129-85/29, 1985

/8/ Cox, C. R., "Development of Piloting Techniques to Reduce Helicopter Approach Noise", 40th Annual Forum of the American Helicopter Society, Arlington/Va., May. 1984, Paper No. A-84-40-04-D000

/9/ Spettstößer, W. R.; Anders, K. P.; Spiegel, K.-H., "Schallmessungen an der Hubschrauberneuentwicklung BK 117 - Bewertete Lärmpegel und Einfluß der Fluggeschwindigkeit", DFVLR-Mitt. 81-18, 1981

/10/ Splettstößer, W. R.; Nagaraja, S. R., "Acoustic Evaluation of the AGUSTA Helicopter 109A in Compliance with the Proposed ICAO ANNEX 16/Chapter 8 Regulations", DFVLR-Mitt. 81-24, 1981

/11/ Splettstößer, W. R.; Heller, H. H.; Klöppel, V., "Helicopter Noise Certification and Sensitivity Studies", 8th European Rotorcraft Forum, Aix-en-Provence, Sep. 1982, Paper No. 9.6

/12/ Splettstößer, W. R; Schultz, K.-J.; Schmitz, F. H.; Boxwell D. A., "Model Rotor High Speed Impulsive Noise - Parametric Variations and Full-Scale Comparisons", Paper 39th Annual National Forum of the American Helicopter Society, St. Louis, Mo., May. 1983

/13/ Boxwell, D. A.; Schmitz, F. H.; Splettstößer, W. R.; Schultz K.-J., "Model Helicopter Rotor High Speed Impulsive Noise - Measured Acoustics and Blade Pressures"; NASA Technical Memorandum 85850 and USA-AVRADCOM Technical Report-83-A-14,Sep. 1983

/14/ Splettstößer, W. R.; Schultz, K.-J.; Boxwell D. A.; Schmitz, F. H., "Helicopter Model Rotor-Blade Vortex Interaction Impulsive Noise: Scalability and Parametric Variations", Tenth European Rotorcraft Forum, Den Haag, The Netherlands, Aug. 1984, Paper No 18

/15/ Schmitz, F. H.; Boxwell, D. A., "In-flight Farfield Measurement of Helicopter Impulsive Noise", J. of the American Helicopter Society, Vol. 21, No. 4, Oct. 1976

/16/ Boxwell, D. A.; Schmitz, F. H., "Full-scale Measurements of Blade-Vortex Interaction Noise", J. of the American Helicopter Society, Vol 27, No. 4, Oct. 1982

/17/ Ffowcs-Williams, J. E. S.; Hawkins D. L., "Sound Generation by Turbulence and Surfaces in Arbitrary Motion", Phil. Trans. of the Royal Society of London, Series A, Vol 264, 1969

ABBREVIATIONS

BMV	German Ministry of Transportation
BVI	Blade/Vortex-Interaction
CAEP	(ICAO-) Committee on Aviation Environmental Protection
DFVLR	German Aerospace Establishment
DNW	German Dutch Wind Tunnel
EPNL	Effective Perceived Noise Level
FAA	(US-) Federal Aviation Administration
HTM	Helical Blade-tip Mach-number
LA	A-weighted Noise Level
ICAO	International Civil Aviation Organization
NASA	US National Air- and Space Administration
NLR	Dutch National Air- and Space Laboratory
OASPL	Overall Sound Pressure Level
PNLT	Tone-corrected Perceived Noise Level
R/C	Rate of Climb
R/D	Rate of Descent
RWTS	Rotary Wing Test Stand

ACKNOWLEDGEMENT

The support and assistance of the management and staff of DNW in the conductance of the research-projects described in this paper are greatly appreciated. Photos courtesy of DNW (Schlieske).